EMBO reports

scientific report

Locating ligand binding and activation of a single antiporter

Alexej Kedrov[1], Michael Krieg[1], Christine Ziegler[2], Werner Kuhlbrandt[2] & Daniel J. Muller[1+]

[1]BIOTEC, University of Technology, Dresden, Germany, and [2]Max Plank Institute of Biophysics, Frankfurt/Main, Germany

Single-molecule force spectroscopy was applied to unfold individual Na^+/H^+ antiporters NhaA from membrane patches. The force–extension curves contained detailed information about the strength and location of molecular interactions established within NhaA. Although molecular interactions that stabilize secondary structure elements remained unaffected on switching NhaA into its functional state, those that are assigned to the Na^+-binding site changed markedly. These interactions were formed only in the presence of Na^+, with their full strength being established at $pH \approx 6$. This finding is in apparent contrast to measurements that suggest that NhaA is fully active at pH 7. Statistical analysis, however, showed that not all NhaA molecules activated this molecular interaction at pH 6, but at pH 7. This implies that the molecular interactions established on Na^+ binding may represent an early step in NhaA activation. The direct observation of molecular interactions established within an antiporter provides new insights into their activation mechanisms.

Keywords: atomic force microscopy; molecular interactions; NhaA; pH activation

EMBO reports advance online publication 17 June 2005;
doi:10.1038/sj.embor.7400455

INTRODUCTION

Na^+/H^+ antiporters are a ubiquitous family of transport membrane proteins found in all cell types, from bacteria to higher plants and mammals, and are essential for the regulation of intracellular pH, Na^+ concentration and cell volume (Padan *et al*, 2001). As antiporters have key roles in human health and disease (Karmazyn *et al*, 1999), they have been the subject of numerous studies during the past decade (Rothman *et al*, 1996; Williams, 2000). In *Escherichia coli*, two antiporters, NhaA and NhaB, specifically exchange Na^+ and Li^+ ions for H^+, allowing the cell to adapt to high environmental salinity and to grow at alkaline pH (Padan *et al*, 2001). NhaA activity is highly dependent on intracellular pH and increases 2,000-fold on increasing the pH from 7.0 to 8.0 (Taglicht *et al*, 1991). No pH dependence was observed for NhaB, implying that NhaA is crucial for cell survival at extreme ambient conditions. Intensive biochemical studies showed distinct amino acids (aa) that were involved in protein function and located within various structural regions of NhaA (Gerchman *et al*, 1993; Rimon *et al*, 1998; Tzubery *et al*, 2004). Moreover, structural changes of extramembrane NhaA domains were detected on protein activation (Rothman *et al*, 1997; Gerchman *et al*, 1999; Venturi *et al*, 2000). However, the ion-transport mechanism of NhaA is not clear as yet because of the lack of sufficient information about the interactions of structural domains. Although the atomic structure of the protein is not resolved, cryo-electron microscopy (cryo-EM) crystallography showed that NhaA consists of 12 α-helices embedded in a lipid bilayer, forming the architectural framework of a channel for ion transportation (Williams *et al*, 1999; Williams, 2000). It was recently shown that helices IV, V and XI are involved in antiporter activity and that certain aa residues are crucial for the proper functioning of NhaA (Galili *et al*, 2002, 2004).

Recently, we combined high-resolution atomic force microscopy (AFM) imaging and single-molecule force spectroscopy to characterize surface structures and molecular interactions of NhaA from *E. coli* (Kedrov *et al*, 2004). The dimeric state of the antiporter and the two-dimensional (2D) crystalline assembly were clearly observed. After imaging, single NhaA molecules were investigated using force spectroscopy. Similarly to the data obtained earlier on bacteriorhodopsin (Oesterhelt *et al*, 2000; Muller *et al*, 2002), aquaporin-I (Moller *et al*, 2003) and halorhodopsin (Cisneros *et al*, 2005), the mechanical unfolding of NhaA was described as a stepwise process in which structural segments showed sufficient mechanical stability to establish unfolding barriers. As soon as the externally applied force superseded the stability of such a structural segment, all aa of the domain unfolded cooperatively (Fig 1A). These unfolding barriers denote the presence of sufficiently strong interactions within the protein structure (Fig 1A) that stabilize individual helices, loops or fragments within it (Kedrov *et al*, 2004; Cisneros *et al*, 2005).

The characteristic unfolding spectra of NhaA contained sets of intensive force peaks (Fig 1A). To assign the structural segments that formed stable units within the protein (Fig 1B, uniformly shaded grey segments), each force peak was fitted using the worm-like chain (WLC) model (Fig 1A, red lines). The fit showed the

[1]BIOTEC, University of Technology, Tatzberg 47, 01062 Dresden, Germany
[2]Max Plank Institute of Biophysics, Max-Laue-Str 3, 60439 Frankfurt/Main, Germany
[+]Corresponding author. Tel: +49 351 46340330; Fax: +49 351 46340342;
E-mail: mueller@biotec.tu-dresden.de

Received 17 January 2005; revised 10 May 2005; accepted 17 May 2005; published online 17 June 2005

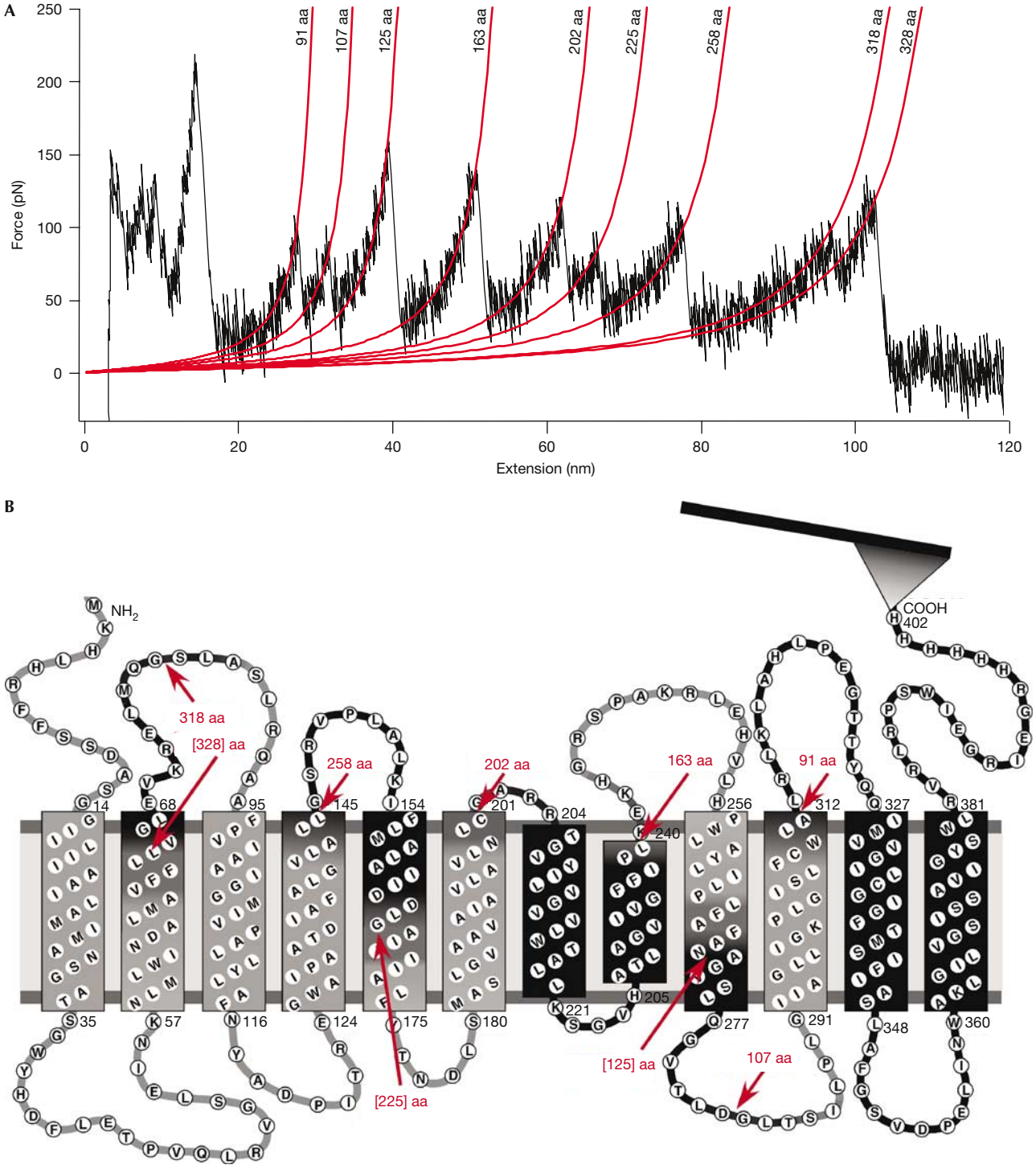

Fig 1 | Mechanical unfolding of a single NhaA molecule. (**A**) Representative force–extension curve recorded on mechanical unfolding of a single NhaA molecule. Each force peak is fitted by the worm-like chain model (red curves), which provides the number of amino-acid (aa) residues stretched. This information was used to assign ends of structural segments (**B**, red arrows) stabilized by molecular interactions. (**B**) Secondary structure of NhaA mapped with stable structural segments detected on pulling the carboxyl terminus. Individual structural segments were uniformly shaded grey, whereas the grey gradients reflect uncertainties in determining segment ends. To determine merges of the segments opposite to the atomic force microscopy tip side of the membrane, or within, a membrane thickness of 4 nm was considered. Their corresponding contour lengths are given in brackets (Kedrov *et al*, 2004).

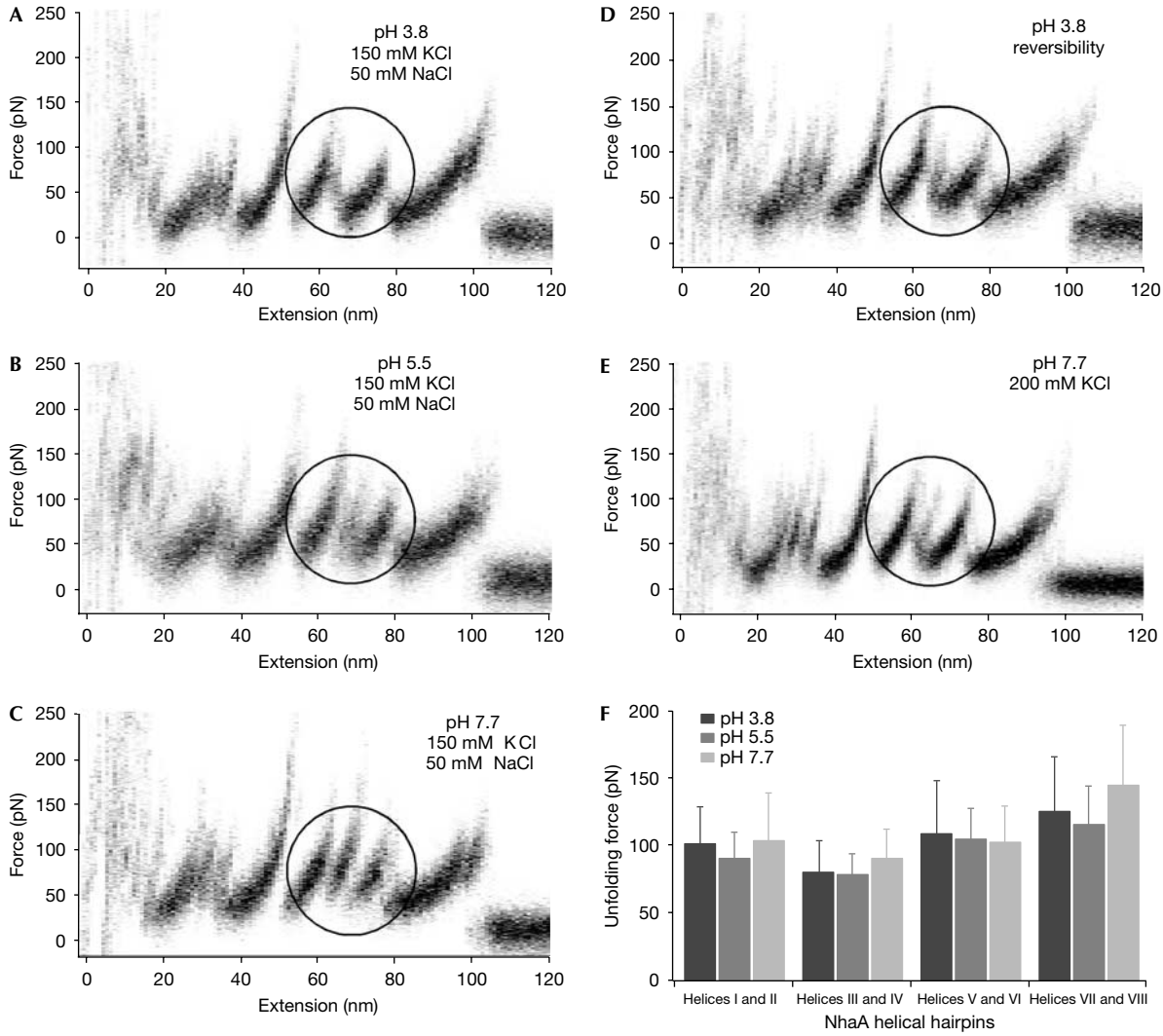

Fig 2 | Detection of pH and Na^+ dependence of molecular interactions established within NhaA. Superimpositions of force–extension curves recorded on single NhaA unfolding at (**A**) pH 3.8 and (**B**) pH 5.5 (inactive states) and (**C**) pH 7.7 (active state) at electrolyte concentrations of 150mM KCl and 50mM NaCl. The pH-dependent unfolding peak at 225 amino acids (aa) is encircled. To prove the reversibility of the pH-dependent change, NhaA was incubated for 1 h at pH 7.7 and unfolded at pH 3.8 (**D**). Significant restoration of the protein stability suggests the reversibility of molecular interactions. (**E**) Force–extension curves of NhaA recorded at pH 7.7 in the absence of NaCl reduced the molecular interaction to that measured for the inactive state. A total of 20 force–extension curves were superimposed for each figure. (**F**) Average unfolding forces of helical pairs. Forces and standard deviations are plotted for different pH values at 150 mM KCl and 50 mM NaCl. Pairs of neighbouring helices tend to unfold cooperatively, giving force peaks at 163 aa (helices VII and VIII), 202 aa (helices V and VI), 258 aa (helices III and IV) and 328 aa (helices I and II; Kedrov *et al*, 2004).

length of the stretched polypeptide and allowed the polypeptide regions that formed stable entities to be assigned. However, the unfolding of individual NhaA molecules showed that their force spectra could vary from each other. Although some peaks occurred with almost 100% probability, others had a much lower probability. This difference of the force spectra reflected the different unfolding pathways of NhaA (Kedrov *et al*, 2004).

Owing to its high sensitivity, single-molecule force spectroscopy has been proposed as a potential tool for probing different conformational states of single biological macromolecules (Albrecht *et al*, 2003), and for screening molecular interactions that stabilize membrane proteins over a range of environmental factors (Muller *et al*, 2002; Janovjak *et al*, 2003). We consider NhaA as an extremely interesting protein for such a study, as it is triggered by pH and switches from an inactive to a fully functional state within 1 pH unit (Taglicht *et al*, 1991). This mechanism is of fundamental importance for proper cell response at different environmental conditions and is relevant for different cell types (Wakabayashi *et al*, 1997; Padan *et al*, 2001). To characterize molecular forces that drive different functional forms of NhaA, we unfolded the

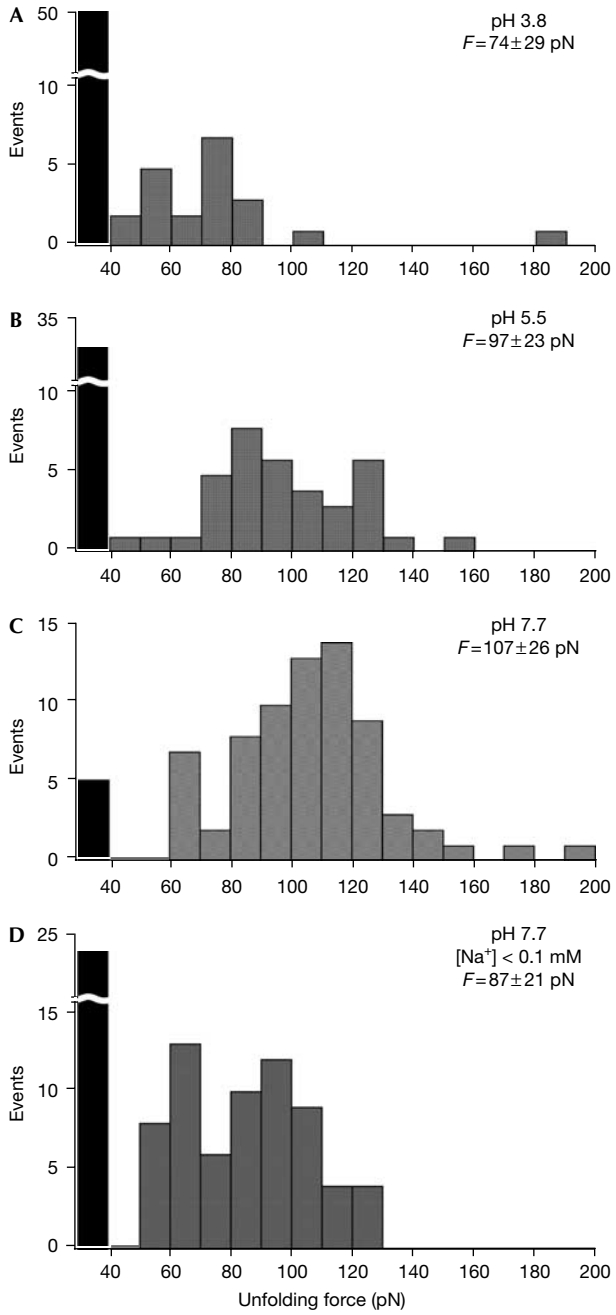

Fig 3 | pH- and Na^+-dependent molecular interactions established at the active site of NhaA. Change in the stability of helix V derived from single-molecule unfolding events is shown. Distribution of unfolding forces of helix V (peak 225 amino acids (aa)) in the presence of Na^+ is given by histograms for pH 3.8 (**A**), 5.5 (**B**) and 7.7 (**C**). (**D**) Removal of Na^+ ions from the buffer solution reduced the molecular interaction to that measured for inactive NhaA (**A**,**B**). About 70 single-molecule unfolding spectra were analysed at each pH (see the Methods). Distributions **A** and **C**, **C** and **D** are statistically different with a significance of $P<0.001$. Black bars on the left of the histograms represent unfolding events in which no peak was detected at 225 aa.

protein in a pH range between 3.8 and 7.7, using single-molecule force spectroscopy. The data show that on increasing the pH to 7 and with simultaneous Na^+ binding, NhaA establishes molecular interactions that are essential for its functional cycle.

RESULTS AND DISCUSSION

NhaA remains fully folded over a wide pH range

Fig 2A–C shows superimpositions of force–extension curves recorded on unfolding individual NhaA molecules at different pH values. They correspond to unfolding of inactive (pH 3.8 and 5.5) and fully active (pH 7.7) forms of NhaA (Taglicht *et al*, 1991). All superimpositions show the characteristic unfolding spectra of NhaA as reported (Kedrov *et al*, 2004) and show no additional unfolding events. The unfolding peaks allowed the location of structural segments that formed unfolding barriers (Fig 1A). Average forces required to unfold helical pairs I and II, III and IV, V and VI, and VII and VIII (Fig 2F) show that their stability is retained independent of the pH range of 3.8–7.7. Both the unaffected stability and locations of molecular interactions that stabilize the structural domains of NhaA imply that they do not change on protein activation. Hence, it can be concluded that the protein maintained its folded stable conformation in the experiments.

Helix V establishes molecular interactions

Although the general profile of the unfolding curves of NhaA remained unchanged on pH variation, the molecular interactions establishing the force peak 225 aa increased significantly (Fig 2A–C, encircled areas). On the basis of the primary and presumed secondary structure of NhaA (Rothman *et al*, 1996), we recently showed that the corresponding unfolding barrier was located in the middle of transmembrane helix V (Fig 1; Kedrov *et al*, 2004). Overcoming the molecular interactions that stabilize this structural region by an externally applied force induces unfolding of the cytoplasmic half of helix V. On raising the pH from 3.8 to 7.7, the average force required to overcome the molecular interactions increased from 74 ± 29 to 107 ± 26 pN (average$\pm$s.d.). Thus, in fully active NhaA, the molecular interactions established within this region reached the strength typically measured for unfolding of a helical pair (Figs 2F,4A). Simultaneously, the frequency of peak detection increased from 31% to 94% (Fig 4B). Detailed insights into the kinetics of this local stabilization were achieved by analysing single-molecule unfolding events (Fig 3A–C). The histograms of the unfolding force distribution clearly show an increased frequency of the 225 aa peak when approaching functional pH values. The increased stability of this region shifted the force distribution gradually to $\sim$100–120 pN. Reversing the pH from 7.7 to 3.8 restored initial molecular interactions (Fig 2D), as the mean unfolding force reduced to values (78 ± 30 pN) similar to those detected for the inactive form of NhaA (74 ± 29 pN).

Location and activation of ligand-binding site

Several studies on NhaA imply that the negatively charged aspartic acid residues 163 and 164 are involved in the Na^+-binding site located in the centre of transmembrane helix V. Substitution of these residues with cysteines or asparagines markedly reduced the cation-transport activity of NhaA (Inoue *et al*, 1995; Padan *et al*, 2001). It has been shown for different

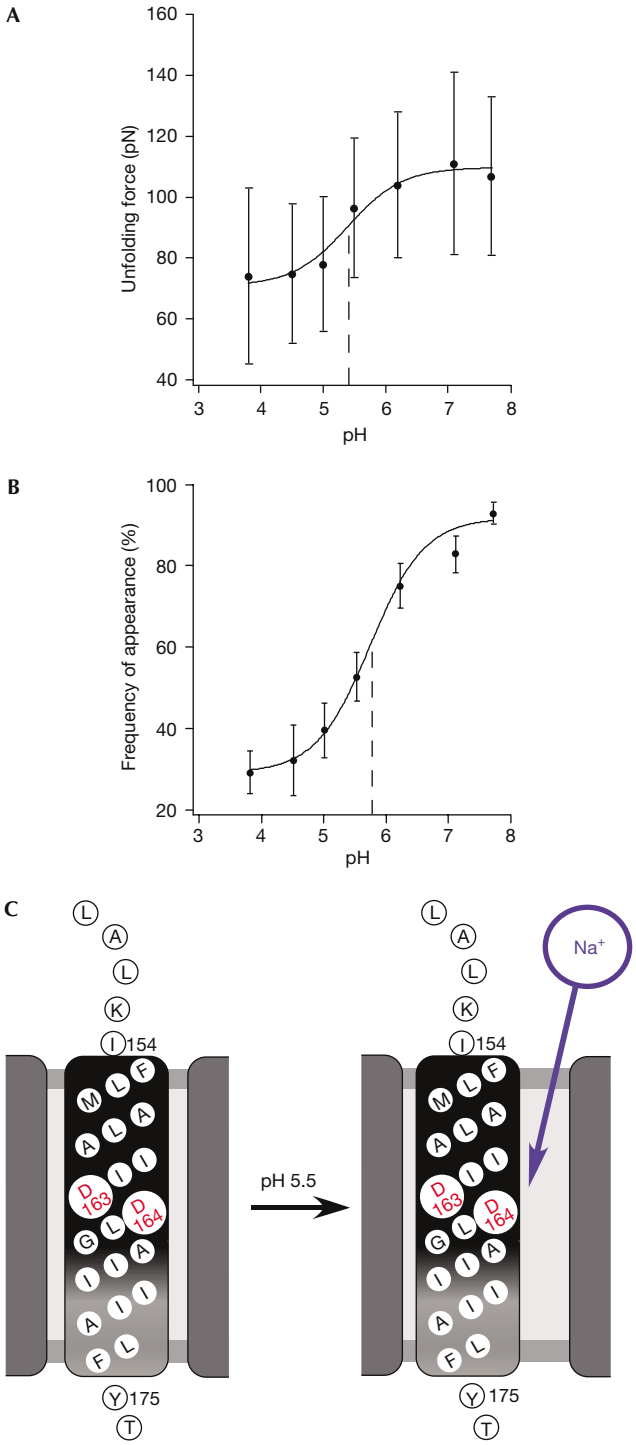

Fig 4 | Characterization of molecular forces established at the ligand-binding site of NhaA. Strength (**A**) and frequency (**B**) of molecular interactions established at the ligand-binding site (**C**) increase on changing pH from 5 to 6. Solid lines represent sigmoid fits of the data points. Dashed lines indicate pH values at which the midpoints of transitions were reached. (**C**) Primary and secondary structures of helix V. Aspartic acids (D163 and 164) of the Na^+-binding site are indicated. pH changes enable accessibility of Na^+ ions.

membrane proteins that ligand binding during the functional cycle can alter the protein conformation (Wang *et al*, 1997; Ferguson *et al*, 2002; le Coutre *et al*, 2002), causing changes in molecular interactions. As the observed change in interactions is localized in the direct proximity of the ligand-binding site of NhaA, we applied force spectroscopy to probe the effect of Na^+ ions on this site. For this purpose, we unfolded single NhaA molecules at pH 7.7 in the absence of NaCl (Fig 2E). To eliminate possible effects of nonspecific electrostatic interactions, the total ionic strength of the buffer solution was kept constant, using KCl as substitute. The force experiments did not detect any change of the unfolding pathways in the absence of Na^+ ions except for the 225 aa peak, which almost disappeared. Moreover, the distribution of unfolding forces (Fig 3D) showed two peaks at 60–70 and 90–100 pN. The peak at 90–100 pN suggested that a certain fraction of the molecules (30–35%) still possessed strong molecular interactions within helix V. The specificity of Na^+ ions strongly suggests that they have an important role in establishing the molecular interactions at the ligand-binding site of helix V. Together with the observed pH-dependent formation of these interactions, it may be suggested that the accessibility of the binding site to Na^+ ions is governed by pH. It is assumed that this ion-binding capability may be altered with small changes of the side-chain orientation (Wang *et al*, 1997), which is promoted by minute spatial rearrangements of the NhaA helices. Thus, we conclude that the antiporter is activated by intramolecular interactions, which are established only at neutral pH, and simultaneously occurring ligand binding.

Strength and probability of molecular interactions

To analyse formation and kinetics of molecular interactions that were established on NhaA activation, the frequency of peak appearance at aa 225 and rupture forces were measured at pH values ranging from 3.8 to 7.7. The data suggested that the interactions gradually increased when the pH was increased from 5 to 6 (Fig 4A). Also, the probability of the peak appearance continuously increased with the pH (Fig 4B). It showed, however, a much lower slope beginning at pH 4 (~30%) and finally reaching ~95% at pH 7.5. Sigmoid distributions (Fig 4A,B, black curves) accurately fitted (equation (1)) the data points assuming $C_1 = 39$, $C_2 = 70$ for force and $C_1 = 29$, $C_2 = 63$ for probability. Midpoints of both transitions were located at $pH_0 = 5.4$ (force) and 5.7 (probability). Clearly, both midpoints for establishing the molecular interactions were shifted to the acidic range, compared with pH 7.5, the optimum reported for NhaA activity (Taglicht *et al*, 1991). One possible explanation could be that the observed formation of molecular interactions within transmembrane helix V relates to an early activation step of the protein, whereas previously reported structural changes (Rothman *et al*, 1997; Venturi *et al*, 2000) finalize the activation of the antiporter at pH range 7–8. The full activity of NhaA would then be reached at pH 7.5, the value at which the molecular interactions at the active site of the protein reached their full strength and occurred with a probability of >90%. Thus, we conclude that establishing the full strength of molecular interactions constitutes an initial step towards activating a single NhaA. These observations are in agreement with those made on lactose permease (Zhang *et al*, 2002; Abramson *et al*, 2003), a paradigmatic secondary transporter (Abramson *et al*, 2004).

The unfolding spectra of membrane proteins significantly depend on the loading rate, which reflects the non-equilibrium nature of the single-molecule experiments. As a result, the frequency of appearance of side peaks can be modulated by pulling speed (Janovjak *et al*, 2004). Thus, we performed additional unfolding experiments on inactive NhaA (pH 3.8) at a higher pulling speed of 1 μm/s, which shifted the frequency of the 225 aa peak to ~65%. In contrast, at pH 7.7, the frequency remained ~95% (data available on request). Remarkably, irrespective of the pulling speed, the molecular interaction centred at aa 225 reached its maximum stability at pH ~ 6. Thus, we assume that changing the pulling speed shifts the slope of the molecular forces and of their probability to occur within the active site of NhaA. The conclusions remained unchanged, however, that the full strength of interactions is established at a pH range before NhaA becomes fully active.

For the first time, single-molecule force spectroscopy has been used to detect molecular interactions that activate the ion-translocation channel of an antiporter. In its active state (pH 7.7), the pH-regulated Na^+/H^+ antiporter NhaA established the full strength of intramolecular interactions, being located at the centre of transmembrane helix V. The proximity of the pH-dependent interactions to the Na^+-binding site of NhaA related these molecular interactions to protein activation. Meanwhile, the stability of other transmembrane helices was not affected by a change in pH. Removal of Na^+ impaired these interactions. Thus, it is concluded that the molecular interactions established within helix V are triggered by pH and Na^+ binding. Complementary to previous biochemical studies on NhaA, our experiments allowed detection and location of changes of molecular interactions that were associated with the structure–function relationship of a membrane protein. We assume that further combination of the applied technique with conventional biophysical techniques, such as electron microscopy or site-directed spin labelling, will allow comprehensive study of how molecular interactions drive membrane protein structure and dynamics.

METHODS

Atomic force microscopy. The AFM used (Nanoscope IIIa) was equipped with a fluid cell and 200-μm-long Si_3N_4 AFM cantilevers (di-Veeco, USA). Spring constants of cantilevers were determined (≈0.06 N/m) using the equipartition theorem (Butt, 1995; Florin *et al*, 1995). 2D crystals of NhaA were immobilized on freshly cleaved mica in 150 mM KCl, 10% glycerol and 25 mM Ka^+-acetate (pH 4) for 20 min. Experiments were performed in buffer solutions containing 150 mM KCl and 50 mM NaCl at pH 3.8 (20 mM citric acid), 4.5 (20 mM K^+-acetate), 5.0 (20 mM citric acid), 5.5 (20 mM MES), 6.3 (20 mM HEPES), 7.1 (20 mM HEPES) and 7.7 (20 mM Tris). Na^+-free buffers contained less than 0.1 mM Na^+ as estimated by atomic absorption spectroscopy. All buffer solutions were made in fresh nano-pure water (18.2 MΩ cm), using reagents of p.a. purity grade from Sigma/Merck (Darmstadt, Germany). On buffer exchange, the set-up was equilibrated for 30 min. After AFM imaging of immobilized crystal patches (Kedrov *et al*, 2004), an undisturbed area was selected to unfold individual proteins. The AFM tip was then brought in contact with the protein applying a force of 0.5–1 nN to attach its terminal end. After 1 s, the tip was withdrawn from the membrane at 120 nm/s, while cantilever deflection was detected. The value of the deflection at each time point was used to calculate the force acting on the molecule using Hook's law.

Data analysis. Pulling NhaA (402 aa) from either the amino or carboxyl terminus yielded characteristic force–extension curves, each showing a length of ~100 nm (Kedrov *et al*, 2004). In this study, we focused on C-terminal unfolding events because of the marked decrease in the frequency of N-terminal unfolding events observed at higher pH. Force–extension curves recorded on single-protein unfolding were manually superimposed. To obtain the unfolded polypeptide chain length, each peak was fitted using the WLC model (Bustamante *et al*, 1994), as described (Kedrov *et al*, 2004).

Per cent probability and average unfolding forces were calculated for each force peak. The standard error of the mean frequency value was derived from the binomial distribution. We analysed 74 (pH 3.8), 43 (pH 4.5), 60 (pH 5.0), 70 (pH 5.5), 59 (pH 6.2), 68 (pH 7.1) and 74 (pH 7.7) events at the pH indicated. Distributions of unfolding force and per cent probabilities versus pH were fitted using the sigmoid function described by

$$f(\mathrm{pH}) = C_1 + \frac{C_2}{1 + \log^{-(\mathrm{pH}-\mathrm{pH}_0)}} \qquad (1)$$

C_1 and C_2 determine the limits of the function at low and high pH values, and pH_0 is the midpoint of transition.

Supplementary information is available at *EMBO reports* online (http://www.emboreports.org).

ACKNOWLEDGEMENTS

We thank E. Padan, H. Janovjak and T. Sapra for valuable discussions. This work was supported by Deutsche Forschungsgemeinschaft (DFG), Volkswagenstiftung, Free State of Saxony and EU.

REFERENCES

Abramson J, Smirnova I, Kasho V, Verner G, Kaback HR, Iwata S (2003) Structure and mechanism of the lactose permease of *Escherichia coli*. *Science* 301: 610–615

Abramson J, Iwata S, Kaback HR (2004) Lactose permease as a paradigm for membrane transport proteins. *Mol Membr Biol* 21: 227–236

Albrecht C, Blank K, Lalic-Multhaler M, Hirler S, Mai T, Gilbert I, Schiffman S, Bayer T, Clausen-Schaumann H, Gaub HE (2003) DNA: a programmable force sensor. *Science* 301: 367–370

Bustamante C, Siggia ED, Smith S (1994) Entropic elasticity of λ-phage DNA. *Science* 265: 1599–1600

Butt HJ (1995) Calculation of thermal noise in atomic force microscopy. *Nanotechnology* 6: 1–7

Cisneros D, Oesterhelt D, Muller DJ (2005) Probing origins of molecular interactions stabilizing the membrane proteins halorodopsin and bacteriorhodopsin. *Structure* 13: 235–242

Ferguson AD, Chakraborty R, Smith BS, Esser L, Helm D, Deisenhofer J (2002) Structural basis of gating by the outer membrane transporter FecA. *Science* 295: 1715–1719

Florin EL, Rief M, Lehmann H, Ludwig M, Dornmair C, Moy VT, Gaub HE (1995) Sensing specific molecular interactions with the atomic force microscopy. *Biosens Bioelectron* 10: 895–901

Galili L, Rothman A, Kozachkov L, Rimon A, Padan E (2002) Trans membrane domain IV is involved in ion transport activity and pH regulation of the NhaA-Na(+)/H(+) antiporter of *Escherichia coli*. *Biochemistry* 41: 609–617

Galili L, Herz K, Dym O, Padan E (2004) Unraveling functional and structural interactions between transmembrane domains IV and XI of NhaA Na^+/H^+ antiporter of *Escherichia coli*. *J Biol Chem* 279: 23104–23113

Gerchman Y, Olami Y, Rimon A, Taglicht D, Schuldiner S, Padan E (1993) Histidine-226 is part of the pH sensor of NhaA, a Na^+/H^+ antiporter in *Escherichia coli*. *Proc Natl Acad Sci USA* 90: 1212–1216

Gerchman Y, Rimon A, Padan E (1999) A pH-dependent conformational change of NhaA Na(+)/H(+) antiporter of *Escherichia coli* involves loop VIII–IX, plays a role in the pH response of the protein, and is maintained by the pure protein in dodecyl maltoside. *J Biol Chem* **274**: 24617–24624

Inoue H, Noumi T, Tsuchiya T, Kanazawa H (1995) Essential aspartic acid residues, Asp-133, Asp-163 and Asp-164, in the transmembrane helices of a Na^+/H^+ antiporter (NhaA) from *Escherichia coli*. *FEBS Lett* **363**: 264–268

Janovjak H, Kessler M, Oesterhelt D, Gaub H, Muller DJ (2003) Unfolding pathways of native bacteriorhodopsin depend on temperature. *EMBO J* **22**: 5220–5229

Janovjak H, Struckmeier J, Hubain M, Kedrov A, Kessler M, Muller DJ (2004) Probing the energy landscape of the membrane protein bacteriorhodopsin. *Structure* **12**: 871–879

Karmazyn M, Gan XT, Humphreys RA, Yoshida H, Kusumoto K (1999) The myocardial Na(+)–H(+) exchange: structure, regulation, and its role in heart disease. *Circ Res* **85**: 777–786

Kedrov A, Ziegler C, Janovjak H, Kuhlbrandt W, Muller DJ (2004) Controlled unfolding and refolding of a single sodium-proton antiporter using atomic force microscopy. *J Mol Biol* **340**: 1143–1152

le Coutre J, Turk E, Kaback HR, Wright EM (2002) Ligand-induced differences in secondary structure of the *Vibrio parahaemolyticus* Na^+/galactose cotransporter. *Biochemistry* **41**: 8082–8086

Moller C, Fotiadis D, Suda K, Engel A, Kessler M, Muller DJ (2003) Determining molecular forces that stabilize human aquaporin-1. *J Struct Biol* **142**: 369–378

Muller DJ, Kessler M, Oesterhelt F, Moller C, Oesterhelt D, Gaub H (2002) Stability of bacteriorhodopsin α-helices and loops analyzed by single-molecule force spectroscopy. *Biophys J* **83**: 3578–3588

Oesterhelt F, Oesterhelt D, Pfeiffer M, Engel A, Gaub HE, Muller DJ (2000) Unfolding pathways of individual bacteriorhodopsins. *Science* **288**: 143–146

Padan E, Venturi M, Gerchman Y, Dover N (2001) Na(+)/H(+) antiporters. *Biochim Biophys Acta* **1505**: 144–157

Rimon A, Gerchman Y, Kariv Z, Padan E (1998) A point mutation (G338S) and its suppressor mutations affect both the pH response of the NhaA-Na^+/H^+ antiporter as well as the growth phenotype of *Escherichia coli*. *J Biol Chem* **273**: 26470–26476

Rothman A, Padan E, Schuldiner S (1996) Topological analysis of NhaA, a Na^+/H^+ antiporter from *Escherichia coli*. *J Biol Chem* **271**: 32288–32292

Rothman A, Gerchman Y, Padan E, Schuldiner S (1997) Probing the conformation of NhaA, a Na^+/H^+ antiporter from *Escherichia coli*, with trypsin. *Biochemistry* **36**: 14572–14576

Taglicht D, Padan E, Schuldiner S (1991) Overproduction and purification of a functional Na^+/H^+ antiporter coded by nhaA (ant) from *Escherichia coli*. *J Biol Chem* **266**: 11289–11294

Tzubery T, Rimon A, Padan E (2004) Mutation E252C increases drastically the K_m value for Na^+ and causes an alkaline shift of the pH dependence of NhaA Na^+/H^+ antiporter of *Escherichia coli*. *J Biol Chem* **279**: 3265–3272

Venturi M, Rimon A, Gerchman Y, Hunte C, Padan E, Michel H (2000) The monoclonal antibody 1F6 identifies a pH-dependent conformational change in the hydrophilic NH(2) terminus of NhaA Na(+)/H(+) antiporter of *Escherichia coli*. *J Biol Chem* **275**: 4734–4742

Wakabayashi S, Shigekawa M, Pouyssegur J (1997) Molecular physiology of vertebrate Na^+/H^+ exchangers. *Physiol Rev* **77**: 51–74

Wang Q, Matsushita K, de Foresta B, le Maire M, Kaback HR (1997) Ligand-induced movement of helix X in the lactose permease from *E. coli*: a fluorescence quenching study. *Biochemistry* **36**: 14120–14127

Williams KA (2000) Three-dimensional structure of the ion-coupled transport protein NhaA. *Nature* **403**: 112–115

Williams KA, Geldmacher-Kaufer U, Padan E, Schuldiner S, Kuhlbrandt W (1999) Projection structure of NhaA, a secondary transporter from *Escherichia coli*, at 4.0 Å resolution. *EMBO J* **18**: 3558–3563

Zhang W, Guan L, Kaback HR (2002) Helices VII and X in the lactose permease of *Escherichia coli*: proximity and ligand-induced distance changes. *J Mol Biol* **315**: 53–62